

Serine Phosphorylation Negatively Regulates RhoA *in Vivo**

Received for publication, December 20, 2002, and in revised form, March 20, 2003
Published, JBC Papers in Press, March 24, 2003, DOI 10.1074/jbc.M213066200

Shawn M. Ellerbroek^{‡§}, Krister Wennerberg^{‡¶}, and Keith Burridge[‡]

From the Departments of [‡]Cell and Developmental Biology and [¶]Pharmacology, Lineberger Comprehensive Cancer Center, University of North Carolina, Chapel Hill, North Carolina 27599

Previous work indicates that RhoA phosphorylation on Ser¹⁸⁸ by cAMP or cGMP-dependent kinases inhibits its activity. However, these studies lacked the possibility to directly study phosphorylated RhoA activity *in vivo*. Therefore, we created RhoA proteins containing phosphomimetic residues in place of the cAMP/cGMP-dependent kinase phosphorylation site. RhoA phosphorylation or phosphomimetic substitution did not affect Rho guanine nucleotide exchange factor, GTPase activating protein, or geranylgeranyl transferase activity *in vitro* but promoted binding to the Rho guanine-dissociation inhibitor as measured by exchange factor competition assays. The *in vitro* similarities between RhoA phosphomimetic proteins and phosphorylated RhoA allowed us to study function of phosphorylated RhoA *in vivo*. RhoA phosphomimetic proteins display depressed GTP loading when transiently expressed in NIH 3T3 cells. Stable-expressing RhoA and RhoA(S188A) clones spread significantly slower than mock-transfected or RhoA(S188E) clones. RhoA(S188A) clones were protected from the morphological effects of a cAMP agonist, whereas phosphomimetic clones exhibit stress fiber disassembly similar to control cells. Together, these data provide *in vivo* evidence that addition of a charged group to Ser¹⁸⁸ upon phosphorylation negatively regulates RhoA activity and indicates that this occurs through enhanced Rho guanine-dissociation inhibitor interaction rather than direct perturbation of guanine nucleotide exchange factor, GTPase activating protein, or geranylgeranyl transferase activity.

The intracellular protein RhoA, a member of the Ras superfamily of low molecular weight G proteins, regulates cell cycle progression, gene expression, focal adhesion assembly/disassembly, and the acto-myosin generated contraction and tension events of cell motility, matrix remodeling, and cytokinesis (1). RhoA cycles between an active GTP-bound and an inactive GDP-bound state through nucleotide exchange and intrinsic GTPase activity. During cellular events of RhoA activation, guanine nucleotide exchange factors (GEFs)¹ can bind and

activate RhoA by promoting uptake of free nucleotide (2). GTPase activating proteins (GAPs) negatively regulate RhoA by binding and stimulating GTP hydrolysis leading to an inactive GDP-bound state (3). RhoA signals within the cell by binding to a variety of effector molecules, such as mDia and the Rho kinases ROK α /ROCK2 and ROK β /ROCK1 (4–6). The vast majority of RhoA (>95%) resides in the cytosolic fraction of the cell (7, 8), with the remainder associated with lipid membranes via a geranylgeranyl moiety attached to a carboxyl Cys¹⁹⁰ residue (9). Prenylation of RhoA is required for promotion of cell growth, transformation, and cytoskeletal organization, indicating that membrane cycling is a critical component of Rho regulation (10). A primary mechanism of cytosolic sequestration of RhoA is through binding of Rho guanine-dissociation inhibitors (RhoGDIs) (11). RhoGDI contacts RhoA through two distinct domains, a flexible amino-terminal domain that impedes guanine nucleotide dissociation/hydrolysis and a highly folded carboxyl domain that stabilizes the RhoA geranylgeranyl moiety (12). RhoGDI is postulated to extract RhoA from membranes through concerted actions of both domains (11).

Administration of forskolin, an activator of adenylate cyclase, or dibutyryl cAMP to cells stimulates morphological changes that are strikingly similar to those observed upon introduction of the Rho-specific inhibitor C3-transferase (13). From this initial observation, cAMP- and cGMP-dependent kinase (PKA and PKG) were demonstrated to phosphorylate RhoA on Ser¹⁸⁸ (13, 14), thereby joining RhoA with Rap1a and Rap1b as small GTPases regulated by carboxyl PKA phosphorylation (15, 16). Although PKA phosphorylation is linked to Rap activation (17, 18), evidence indicates that it negatively regulates RhoA function. RhoA phosphorylation promotes formation of RhoA-RhoGDI complexes (13, 19) and enhances the ability of RhoGDI to extract RhoA from membranes (13, 20). In support of enhanced RhoGDI binding, the ability of RhoA to cycle from membranes has been linked to cAMP and cGMP signaling within cells (21, 22). Functionally, constitutively active RhoA containing an S188A mutation is more effective in blocking actin dissolution promoted by dibutyryl cAMP (23) or 8-Bromo-cGMP (24), and constitutively active RhoA require a S188A mutation to promote stress fibers in cells co-transfected with constitutively active PKG (14).

On the other hand, the significance of RhoA phosphorylation to PKA/PKG regulation of its signaling is unclear considering recent reports. Thromboxane receptor stimulation promotes RhoA activation through a G α_{13} and a PKA-sensitive pathway(s) (25). Manganello *et al.* (26) demonstrated recently that PKA phosphorylates G α_{13} subunit to promote $\beta\gamma$ subunit uncoupling, thereby effectively shutting down receptor activation

* This work was supported by an American Cancer Society Postdoctoral Fellowship (to S. M. E.), by the Swedish Foundation for International Cooperation in Research and Higher Education (to K. W.), and by National Institutes of Health Grants GM29860 and HL45100 (to K. B.). The costs of publication of this article were defrayed in part by the payment of page charges. This article must therefore be hereby marked "advertisement" in accordance with 18 U.S.C. Section 1734 solely to indicate this fact.

§ To whom correspondence should be addressed: Lineberger Comprehensive Cancer Center, CB 7295, University of North Carolina, Chapel Hill, NC 27599. Tel.: 919-966-1904; Fax: 919-966-1856; E-mail: hawkeye@med.unc.edu.

¹ The abbreviations used are: GEF, guanine nucleotide exchange factor; cPKA, catalytic domain of protein kinase A; GAP, GTPase activating protein; DH, Dbl homology; PH, pleckstrin homology; CRD,

cysteine-rich domain; GST, glutathione S-transferase; mant, N-methylanthraniloyl; RBD, Rho-binding domain of Rhotekin; RhoGDI, Rho guanine-dissociation inhibitor; ggRhoA, geranylgeranylated RhoA; PKA, cAMP-dependent kinase; PKG, cGMP-dependent kinase.

of RhoA. Moreover, PKG inhibited $G\alpha_{13}$ activation of serum response factor transcription by impeding activation of RhoA (27). Notably, PKG also inhibited serum response factor transcriptional activity promoted by constitutively active forms of Rho kinase, protein kinase N, or protein kinase C-related kinase 2, indicating that PKG antagonizes RhoA signaling downstream of effector regulation. Thus, an emerging picture is that PKA/PKG negatively regulates RhoA at multiple levels.

In this work, we expressed Ser¹⁸⁸ phosphomimetic RhoA proteins, in the absence of constitutive RhoA activity and aberrant PKA/PKG signaling, to assess the contribution of PKA phosphorylation to RhoA function. We report here that addition of a charged group to Ser¹⁸⁸ upon phosphorylation negatively regulates RhoA activity *in vivo* and indicates that this occurs through enhanced RhoGDI interaction rather than direct perturbation of GEF, GAP, or geranylgeranyl transferase activity.

EXPERIMENTAL PROCEDURES

Materials—Puromycin, bovine serum albumin, and buffer reagents were acquired from Sigma. Polyvinylidene fluoride membranes were purchased from Millipore. RhoA monoclonal antibodies (clone 55) were purchased from BD Biosciences. NIH 3T3 cells were maintained in growth medium (Dulbecco's modified Eagle's medium supplemented with 10% bovine calf serum (Sigma)).

Constructs—RhoA mutations (S188A, S188D, S188E, C190A) and RhoG mutation (S187A) were created through PCR mutagenesis using the QuikChange mutagenesis kit (Stratagene). Mutations were confirmed by DNA sequencing, and cDNAs were subcloned into either pGEX4T-1 (Amersham Biosciences) or pCMV-Myc (Clontech) using *EcoRI* and *XhoI* restriction sites. pGEX4T-1-RhoGDI (human) was created by subcloning RhoGDI cDNA into pGEX4T-1 using *BamHI* and *EcoRI* restriction sites. pPro-HT-Dbl (DH/PH) was a gift of Dr. K. Rossman, University of North Carolina, Chapel Hill, NC.

Antibody Production—Antibody production and purification was performed by Covance Research Products Inc. Rabbits were immunized with a phosphoserine peptide containing the proximal nine residues of RhoA (RRGKKK_pSGC) thiol bonded to keyhole limpet hemocyanin. Antibodies were isolated by negative affinity purification with immobilized unphosphorylated RhoA peptide followed by positive affinity purification with immobilized phosphorylated RhoA peptide and low/high pH elutions.

Fusion Proteins—GST-Rho fusion proteins (GST, GST-RhoA, GST-RhoG, GST-Cdc42, GST-Rac1, GST-RhoGDI) were purified from BL21 *Escherichia coli* cells (Stratagene) using glutathione-Sepharose 4B (Amersham Biosciences). Proteins were eluted with free and reduced glutathione in Tris-buffered saline medium (50 mM Tris, 150 mM NaCl, 5 mM MgCl₂, 1 mM dithiothreitol) and stored in 30% glycerol. His₆-Dbl DH/PH was purified from BL21 *E. coli* cells using nickel-nitrilotriacetic acid-Sepharose (Qiagen) and eluted with 20 units of tobacco etch virus protease (Invitrogen) according to the manufacturer's specifications. RhoGDI was produced by cleaving RhoGDI from GST-RhoGDI-Sepharose with 5 units of bovine thrombin (Sigma). RhoGDI was subsequently cleared with benzamidine-agarose (Sigma) to remove thrombin from incubation buffer. Recombinant geranylgeranyl transferase was purchased from Sigma. Phosphate-binding protein carrying an A197C mutation was purified and fluorescently labeled with *N*-[2-1-maleimido]ethyl]-7-(diethylamino)coumarin-3-carboxamide as described previously (28) from *E. coli* ANCC75 bacteria carrying plasmid pSN5182/7 (a kind gift of Dr. M. R. Webb, National Institute for Medical Research, London). His₆-Larg DH/PH and His₆-Vav2 DH/PH/CRD were kind gifts of Dr. M. Booden, University of North Carolina, Chapel Hill, NC. His₆-DH/PH Dbs was a gift of Dr. K. Rossman, University of North Carolina, Chapel Hill, NC. Full-length p190RhoGAP was a generous gift of Dr. J. Settleman, Harvard Medical School.

Rho Protein Phosphorylation—To measure cPKA phosphorylation of Rho fusion proteins (see Fig. 1), 2.0 pmols of fusion proteins, 1.5 units of cPKA (Sigma), 330 pmols of ATP, and 3.3 pmols of [γ -³²P]ATP (Amersham Biosciences) were incubated in phosphorylation buffer (50 mM Tris, 5 mM MgCl₂, 1 mM dithiothreitol) at 30 °C for 20 min. Samples were removed, resolved by 15% SDS-PAGE, and then analyzed by autoradiography of dried gels. For large scale production of phosphorylated GST-RhoA, 120 μ g (2.5 nmols) of GST-RhoA-Sepharose, 150 units of cPKA, and excess ATP (2 mM) were rotated in 1 ml of phosphorylation buffer for 90 min at 25 °C. Phosphorylation efficiency was

estimated by scaling down reaction to 1% the amount of GST-RhoA and cPKA. Specifically, 1.2 μ g (25 pmols) of GST-RhoA-Sepharose, 1.5 units of cPKA, 2.12 nmols of ATP, and 3.3 pmols of [γ -³²P]ATP (1:645 dilution) were incubated in 10 μ l of phosphorylation buffer with rotation for 30 min at 25 °C. Reactions were washed extensively, and incorporation of ³²P was calculated and corrected with values obtained from GST-Sepharose reactions. On average, 0.030–0.035 pmols of ³²P was incorporated by RhoA into each reaction, indicating 80–90% phosphorylation efficiency ((645 \times 0.03 pmol)/25 pmol GST-RhoA). To measure phosphorylation of geranylgeranylated RhoA, 2.0 pmol of unmodified or prenylated RhoA (see below) were incubated with 1.5 units of cPKA, 330 pmols of ATP, and 3.3 pmols of [γ -³²P]ATP in phosphorylation buffer at 30 °C for 20 min. Samples were boiled to stop the reaction and then TX-114 was added to a concentration of 1%, and phase partitioning was performed as described previously for Rho proteins (29). The detergent phase was washed with three 20-fold volumes of phosphate-buffered saline to ensure removal of non-prenylated RhoA. Both aqueous and detergent phases were aliquoted and analyzed for RhoA phosphorylation by measuring release of radioactivity and visualizing by SDS-PAGE and autoradiography.

In Vitro Guanine Nucleotide Exchange Factor Assays—Fluorescence spectroscopic analysis of *N*-methylanthraniloyl (mant)-GTP (Biomol) incorporation into GDP-preloaded GST-Rho proteins was carried out using a FLUOstar fluorescence microplate reader at 25 °C similar to as described previously (30). 2 μ M GST-RhoA or 1 μ M prenylated GST-RhoA was prepared and allowed to equilibrate in exchange buffer (20 mM Tris, pH 7.5, 50 mM NaCl, 10 mM MgCl₂, 1 mM dithiothreitol, 50 μ g/ml bovine serum albumin, 1% glycerol). 500 nM mant-GTP and varying amounts of DH/PH (Larg, Dbl, or Dbs) or DH/PH/CRD (Vav2) protein were added at the indicated time, and the relative mant fluorescence (excitation = 360 nm, emission = 460 nm) was monitored. Experiments were performed in duplicate for every condition.

GAP Assays—GAP assays were performed in a Spectramax Gemini XS fluorescence microplate reader (Molecular Devices) (excitation = 425 nm, emission = 465 nm) at 25 °C by incubating 1 μ M GTP-loaded GST-RhoA together with 2.5 μ M fluorophore-labeled phosphate-binding protein in the absence or presence of 250 or 750 pM purified p190RhoGAP in a buffer containing 20 mM Tris, pH 7.6, and 1 mM MgCl₂ at a total volume of 100 μ l. Upon hydrolysis of GTP, the resulting free P_i is bound rapidly (1.36 \times 10⁸ M⁻¹ s⁻¹ at 22 °C) and with high affinity (about 100 nM) by the phosphate-binding protein, resulting in a 13-fold increase in the fluorescence at 465 nm (28). Because of this, the observed change in fluorescence corresponds to the rate and amount of P_i released from the GTPase.

RhoGDI Competition Assays—2 μ M of the indicated GST-RhoA fusion protein was incubated for 10 min in exchange buffer containing 0.5, 1.0, or 2.0 μ M RhoGDI to promote RhoA-RhoGDI complexes. Vav2 DH/PH/CRD and mant-GTP nucleotides were then added and allowed to equilibrate with mixing for 15 s, and the rate of mant-GTP incorporation was measured. Linear velocity of exchange was determined as described previously (31). Briefly, baseline and GEF-induced nucleotide exchange rates were calculated by dividing the change in emission at 460 nm by change in time. Values were averaged and standard deviations were calculated for each reaction. Velocity was considered linear as long as the regression value of the exchange slope was greater than 0.97. Data from these and all other experiments were considered significantly different if the *p* values, as determined by two-tailed *t* tests, were <0.02.

Geranylgeranyl Transferase Assays—GST or the indicated GST-RhoA-Sepharose (5 pmols), 100 pmols of ³H-geranylgeranyl pyrophosphate (PerkinElmer Life Sciences), and 0.36 units of geranylgeranyl transferase were incubated in Tris-buffered saline medium, pH 7.6, for 20 or 60 min. Samples were resolved by 15% SDS-PAGE, and gels were fixed, incubated in Amplify solution (Amersham Biosciences), and then exposed by autoradiography. Alternatively, reactions were collected at 20, 40, 60, and 80 min in duplicate, washed extensively, and placed in scintillation buffer, and the extent of ³H-geranylgeranyl was quantified. To generate geranylgeranylated RhoA for kinetic assays, 50 μ g (1 nmol) of GST-RhoA or phosphorylated GST-RhoA were incubated in solution with geranylgeranyl pyrophosphate (25 nmols) and in the absence or presence of 10 units of geranylgeranyl transferase overnight at 30 °C. Proteins were either GDP-loaded (GEF assays) or GTP-loaded (GAP assays) and eluted with small volumes of free glutathione in Tris-buffered saline containing 0.25% deoxycholate. Through dilutions, reactions contained either 0.025% (GEF) or 0.015% deoxycholate (GAP). Unmodified RhoA (no transferase) was utilized as an experimental control for the influence of prenylation on GTPase activity (see Fig. 5, C and D).

Transfections and Production of Stable Cells—NIH 3T3 fibroblast cells were transfected with the expression vectors indicated in each experiment according to the manufacturer's protocol using LipofectAMINE PLUS (Invitrogen). After introduction of the expression vectors for 3 h, the transfection medium was replaced with growth medium for 16 h. For creation of stable cell lines, NIH 3T3 cells were transfected with 1 μ g of pPUR (Clontech) only or cotransfected with 0.05 μ g of pPUR and 1 μ g of pCMV-Myc RhoA construct and then selected in 10 μ g/ml puromycin (Sigma). Clonal lines were established and screened for expression by Western blotting lysates with anti-c-Myc (clone 9E10; Sigma) monoclonal antibodies.

RhoA GTP Profile Assays—The amount of activated, GTP-bound RhoA protein was measured using a technique similar to the method described by Ren *et al.* (32). Briefly, transfected or stable cells were lysed in 300 μ l of 50 mM Tris, pH 7.4, 10 mM MgCl₂, 500 mM NaCl, 1% Triton X-100, 0.1% SDS, 0.5% deoxycholate, and protease inhibitors. 500–750 μ g of lysates were cleared at 16,000 \times g for 5 min, and the supernatant was rotated for 30 min with 30 μ g of GST-RBD (GST fusion protein containing the Rho-binding domain (RBD; amino acids 7–89) of Rhotekin) bound to glutathione-Sepharose beads. Samples were washed in 50 mM Tris, pH 7.4, 10 mM MgCl₂, 150 mM NaCl, 1% Triton X-100, and protease inhibitors. GST-RBD pull-downs and lysates were then Western blotted with anti-c-Myc. To quantify GST-RBD pull-downs, Western blots of lysates and corresponding GST-RBD pull-downs from three unique experiments done in duplicate were scanned, and densitometry was performed using Metamorph imaging software.

Calculation of Cell Spreading—For all experiments cells were replated in the absence of puromycin the day before experiments, trypsinized, washed twice in Dulbecco's modified Eagle's medium, and then suspended before plating for 30 min in Dulbecco's modified Eagle's medium and 0.5% fatty acid-free bovine serum albumin. Suspended cells were plated on fibronectin-coated coverslips for 20, 40, and 60 min. Coverslips were fixed and stained with Coomassie Blue (2% Brilliant Blue, 45% methanol, and 10% acetic acid) for 10 min and then washed with water and mounted. The relative areas of individual cells from Metamorph images were quantified with the use of NIH Image software. At least 50 cells taken from 10 arbitrary fields were counted from each coverslip, with two coverslips counted for every condition.

Immunofluorescence—Cells were plated and grown overnight on fibronectin-coated glass coverslips in the presence of serum. Cells were washed free of serum with serum-free medium and then incubated in serum-free media containing either Me₂SO vehicle or 25 μ M forskolin (Sigma) for 20 min. Cells were then fixed for 15 min in 3.7% formaldehyde in phosphate-buffered saline permeabilized for 5 min in 0.5% Triton X-100 in phosphate-buffered saline. Filamentous actin was labeled with Texas Red-conjugated phalloidin (Molecular Probes). Images were obtained on an Axiophot microscope (Zeiss) using a MicroMAX 5-MHz cooled CCD camera (Princeton Instrument) and Metamorph Image software (Universal Imaging Corp.).

RESULTS

PKA Phosphorylation of Rho Proteins—We confirmed that PKA phosphorylates RhoA on Ser¹⁸⁸ (Fig. 1A) as described previously (13). Although Forget *et al.* (19) demonstrated that PKA also phosphorylates Cdc42, we found Cdc42 to be a poor substrate for PKA *in vitro*, in agreement with an initial report (33). Further, Rac1 was not phosphorylated, whereas PKA efficiently phosphorylates RhoG on Ser¹⁸⁷ (Fig. 1A), indicating that both RhoA and RhoG carboxyl termini are targets of PKA phosphorylation. The proximity of the Rho prenylation site (residue 190) to the site of PKA phosphorylation prompted us to examine whether prenylation affects PKA phosphorylation. Although RhoA is efficiently prenylated in our reactions (60–80% by molar incorporation of ³H-geranylgeranyl pyrophosphate), phosphorylated RhoA or geranylgeranylated RhoA (ggRhoA) were subjected to TX-114 phase extraction. TX-114 phase extraction partitions prenylated RhoA into the detergent phase because of the hydrophobic modification (29), ensuring that ggRhoA will be specifically examined as a substrate. Phosphorylation efficiency of RhoA and ggRhoA was comparable (Fig. 1, B and C), demonstrating that prenyl modification of RhoA does not impede PKA phosphorylation. To measure cellular RhoA phosphorylation, we generated affinity-purified antibodies that selectively recognize phospho-Ser¹⁸⁸ RhoA (Fig. 2A). Charac-

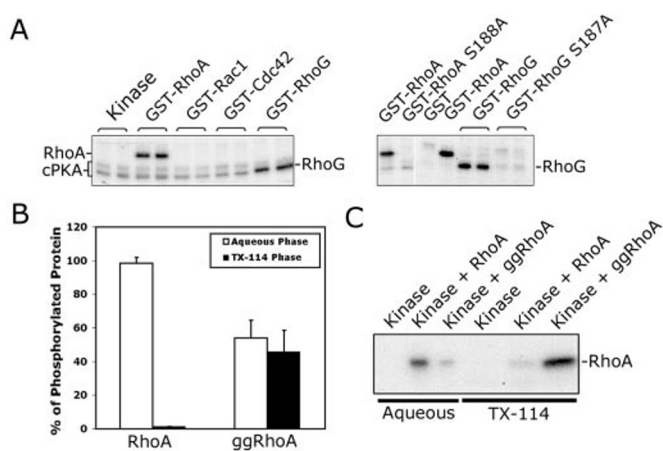


FIG. 1. Characterization of Rho protein phosphorylation. A, GST-Rho fusion proteins were incubated in duplicate, as indicated, with [γ -³²P]ATP and cPKA, and phosphorylation was visualized by SDS-PAGE followed by autoradiography. Mutation of Ser¹⁸⁸ and Ser¹⁸⁷ blocks cPKA phosphorylation of RhoA and RhoG, respectively. B, GST-RhoA was incubated with geranylgeranyl pyrophosphate in the absence or presence of geranylgeranyl transferase to produce control and prenylated RhoA (ggRhoA). RhoA and ggRhoA fusion proteins were phosphorylated with [γ -³²P]ATP and cPKA and then subjected to TX-114 detergent partitioning as described previously (29). Phosphorylation (cpm) of unmodified RhoA, which remains associated with the aqueous phase, and of prenylated RhoA, which partitions into the TX-114 detergent phase, was measured for each reaction. Values are expressed as percent of total amount found in both phases (19,670 cpm for RhoA and 13,796 cpm for ggRhoA \pm S.D.) and were corrected for the low contribution of kinase-bound radioactivity. C, RhoA and ggRhoA phosphorylation were visualized by analyzing 10% of the phase volume or 25% of the TX-114 phase volume by SDS-PAGE followed by autoradiography. TX-114 phase proteins run as wider bands because of the Triton detergent. Phosphorylation of prenylated RhoA was readily evident in the assay, demonstrating that prenylation does not interfere with the catalytic activity of cPKA against Ser¹⁸⁸.

terization of two unique antisera revealed that geranylgeranylation of phosphorylated GST-RhoA proteins abrogated antibody binding (Fig. 2A), indicating that the presence of a C20 isoprenoid moiety sterically blocks antibody recognition. Therefore, we elected to use NIH 3T3 cells that stably express Myc epitope-tagged-RhoA(C190A) to measure cellular PKA phosphorylation of Ser¹⁸⁸. Forskolin stimulation of cAMP production strongly enhanced Myc-RhoA(C190A) phosphorylation as measured by Western blotting of whole cell lysates or immunoprecipitated proteins (Fig. 2B). We and others (32, 34) have established previously that RhoA activity is reduced during the initial 15–30 min of cell spreading. Interestingly, PKA activity is transiently stimulated during the same time course (35). To address whether RhoA is a PKA target during spreading, cells expressing Myc-RhoA(C190A) were allowed to spread on fibronectin and at various times collected for immunoprecipitation with phospho-Ser¹⁸⁸ antibodies. We observed that cellular phosphorylation of RhoA was significantly increased within the initial 20 min of NIH 3T3 cell spreading on fibronectin (Fig. 2C). These data support the conclusion that cellular PKA activity is elevated early in spreading (35, 36) and indicates that RhoA is a target of cellular PKA regulation.

GEF Exchange against Phosphorylated RhoA—GEFs bind GDP-bound Rho proteins and induce a transition state that promotes uptake of free GTP nucleotide, thereby stimulating Rho activation. It has been reported that cAMP inhibits GEF activation of RhoA in leukocytes (37), thereby raising the possibility that RhoA phosphorylation impairs GEF exchange. To address this hypothesis, GST-RhoA was phosphorylated *in vitro* with cPKA and compared with control protein for the ability of DH/PH domain-containing GEFs to promote nucleo-

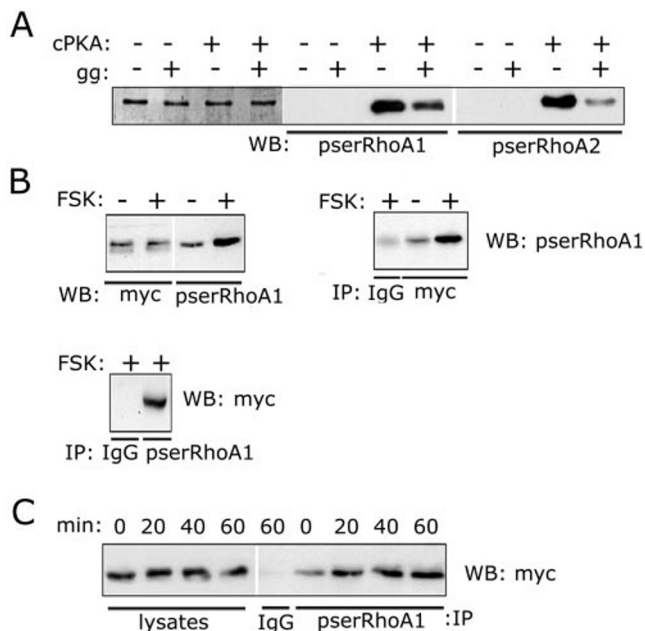


FIG. 2. Intracellular RhoA phosphorylation. *A*, GST-RhoA fusion proteins were phosphorylated by cPKA as indicated and then incubated in the absence or presence of geranylgeranyl (*gg*) transferase. Fusion proteins were either stained by Coomassie or Western blotted (WB) with phospho-Ser¹⁸⁸ RhoA antibodies isolated from two unique sera (*pserRhoA1* and *pserRhoA2*). Antibody recognition was sensitive to the presence of the geranylgeranyl moiety. *B*, NIH 3T3 cells stably expressing Myc-RhoA(C190A) (non-prenylated) were stimulated with 25 μ M forskolin (FSK) for 20 min, and lysates were collected and then Western blotted for recombinant protein (anti-Myc) or RhoA phosphorylation (*pserRhoA1*). Only recombinant Myc-RhoA(C190A) was recognized by *pserRhoA1*. Additionally, cells were treated as above, and Myc-RhoA(C190A) immunoprecipitated (IP) with anti-Myc, anti-*pserRhoA1*, or irrelevant IgG controls as indicated. Western blots of immunoprecipitated material confirm that Myc-RhoA(C190A) is a target of cellular PKA. Background in the IgG control for the Myc immunoprecipitation is from the light chain of mouse IgG, which runs at a similar apparent molecular weight. *C*, to address whether Myc-RhoA(C190A) is a target of PKA during an event of low RhoA activity, cells were allowed to spread on fibronectin for the indicated times, and lysates were collected and immunoprecipitated with either IgG control or *pserRhoA1* antibodies and then Western blotted for the Myc tag. PKA activity and Myc-RhoA(C190A) phosphorylation were increased within 20 min of cell spreading.

uptake. Using [γ -³²P]ATP, GST-RhoA was estimated to be at least 80–90% phosphorylated by cPKA. Basal incorporation of mant-GTP was identical for phosphorylated and control GST-RhoA proteins (Fig. 3A). Larg (Fig. 3A), Vav-2 (Table I), Db1, and Db5 (not shown) all displayed similar exchange activity against control and phosphorylated GST-RhoA at multiple GEF concentrations. This finding also extended to phosphorylated and control geranylgeranylated RhoA proteins (Fig. 3B). Lastly, the phosphomimetics GST-RhoA(S188E) and GST-RhoA(S188D) were equivalent substrates as wild-type GST-RhoA or GST-RhoA(S188A) controls (Fig. 3C). These data demonstrate that phosphorylation of the RhoA tail does not directly interfere with GEF-induced exchange.

RhoA Ser¹⁸⁸ Phosphomimetics Display Increased Binding to RhoGDI—cPKA-phosphorylation of RhoA has been reported to increase its affinity toward RhoGDI, therefore we examined the ability of RhoGDI to bind RhoA proteins using solution-phase binding competition of RhoGDI and GEF molecules. Briefly, GST-RhoA proteins were pre-incubated with no or varying amounts of full-length RhoGDI for 10 min to promote the formation of RhoA-RhoGDI complexes. Vav2 DH/PH/CRD and mant-GTP nucleotides were subsequently added and allowed to equilibrate with mixing for 15 s and then mant-GTP incorpo-

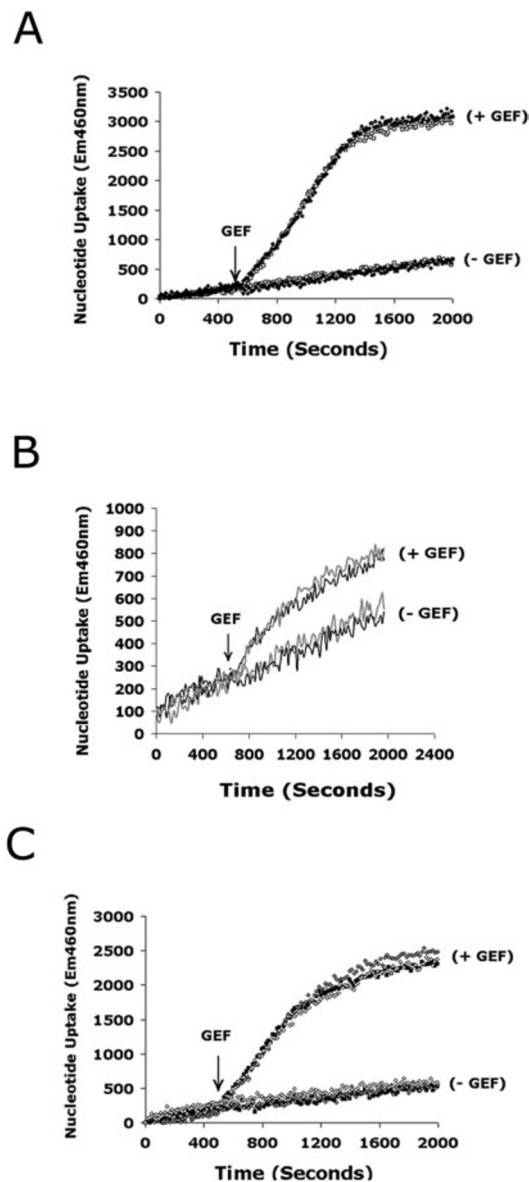


FIG. 3. RhoA phosphorylation does not affect GEF exchange. *A*, phosphorylated or control GST-RhoA were incubated in the presence of mant-GTP before stimulation of exchange by the addition of the Larg DH/PH domain at the indicated time (denoted *GEF* with arrow). Kinetics generated from phosphorylated (*white symbol*) or control proteins (*black symbol*) were indistinguishable. *B*, phosphorylated (*gray curve*) or control (*black curve*) prenylated RhoA was incubated with Vav2 DH/PH/CRD at the indicated time. Vav2 or Larg (not shown) exchange against prenylated RhoA fusion proteins is not affected by PKA phosphorylation of Ser¹⁸⁸. *C*, GST-RhoA (*black symbol*), GST-RhoA(S188A) (*gray symbol*), and GST-RhoA(S188E) (*white symbol*) were treated as above. Larg DH/PH displayed similar activity against GST-RhoA and the GST-RhoA serine mutants.

ration was measured. Vav2 exchange was linear over the initial 150–200 s for phosphorylated, phosphoserine-mimetics, and control GST-RhoA proteins (see Fig. 4A and Tables I and II). As RhoGDI concentrations were increased, the velocity of nucleotide incorporation was both reduced and lengthened for all RhoA molecules (Tables I and II). Importantly, both phosphorylated and phosphomimetic GST-RhoA proteins exhibited a significant reduction in GEF exchange compared with control proteins at equal concentrations of RhoGDI (Fig. 4B). The bulkier S188E mutation resulted in slightly greater inhibition than the S188D mutation, suggesting tighter binding to RhoGDI. As prior experiments demonstrated that GEF ex-

TABLE I

RhoGDI inhibition of GEF-exchange activity (units s⁻¹ ± sd.)

2 μ M phosphorylated or control GST-RhoA proteins were incubated with the indicated amount of RhoGDI (GDI) prior to the addition of Vav2. Linear velocity with standard deviation was calculated as described under "Experimental Procedures." For comparison, -fold induction of nucleotide uptake upon Vav-2 addition (Vav-2 exchange/basal uptake) and the percent inhibition of this induction are provided. RhoGDI inhibition of Vav2-induced nucleotide exchange was more robust for phosphorylated RhoA than control protein.

Condition	RhoA	RhoA-phosphorylated
Basal	0.98 ± 0.15	0.87 ± 0.13
150 nM Vav2	3.84 ± 0.21 (3.9-fold)	3.52 ± 0.27 (4.1-fold)
+ 0.5 μ M GDI	3.08 ± 0.30 (81%)	3.26 ± 0.33 (93%)
+ 1.0 μ M GDI	2.83 ± 0.22 (74%)	2.37 ± 0.34 (67%) ^a
+ 2.0 μ M GDI	2.34 ± 0.28 (61%)	1.51 ± 0.28 (43%) ^a

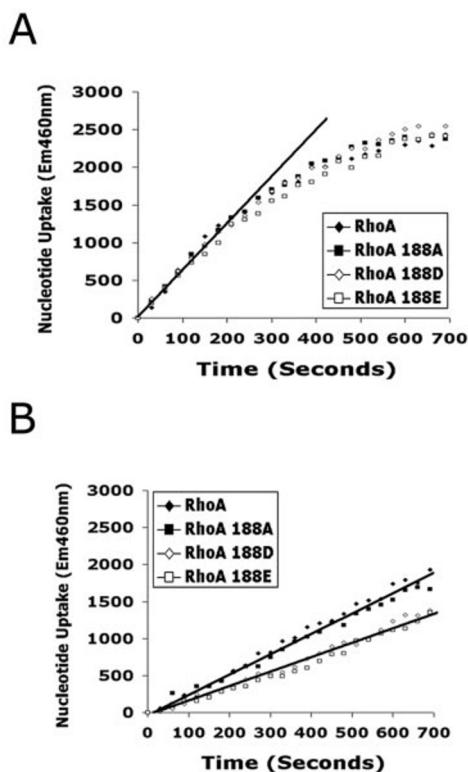
^a *p* < 0.01.

FIG. 4. RhoA phosphorylation promotes RhoGDI interaction. A, GST-RhoA or GST-RhoA serine mutants, as indicated, were allowed to equilibrate for 15 min prior to the addition of the DH/PH/CRD Vav2 and mant-GTP. Vav2 promoted an equivalent linear exchange velocity for all GST-RhoA proteins. B, equal molar amounts of RhoGDI and GST-RhoA proteins (2 μ M) were equilibrated with GST-RhoA proteins for 15 min prior to addition of DH/PH/CRD of Vav2. RhoGDI inhibition of GEF exchanges results in a slower and more sustained linear exchange velocity for all RhoA proteins compared with A. The linear exchange velocities of the two phosphomimetics, GST-RhoA(S188D) and GST-RhoA(S188E), were significantly depressed compared with GST-RhoA and GST-RhoA(S188A) protein controls.

change was equivalent for all RhoA proteins at multiple concentrations, these data provide additional evidence to previous reports that RhoA phosphorylation promotes or stabilizes RhoA-RhoGDI complex formation. Moreover, as these proteins are not post-translationally modified, these data indicate that adding a negative charge to the carboxyl terminus of RhoA enhances the protein-protein interactions of RhoA and RhoGDI.

RhoA Phosphorylation Does Not Affect GAP Activity—RhoGAPs negatively regulate Rho activity by promoting the intrinsic GTP-hydrolyzing activity of Rho proteins. As cPKA phospho-

rylation is also hypothesized to negatively regulate RhoA, we analyzed whether p190RhoGAP activity against phosphorylated RhoA is perturbed *in vitro*. Basal and p190RhoGAP-induced GTP hydrolysis by phosphorylated, phosphoserine-mimetic, and control GST-RhoA proteins was essentially identical (Fig. 5, A and B). Moreover, p190RhoGAP activity against geranylgeranylated RhoA was also insensitive to PKA phosphorylation, although prenylated RhoA had a slightly lower basal and GAP-induced hydrolysis rate (Fig. 5, C and D). Together, these data indicate that phosphorylation of RhoA does not influence the ability of p190RhoGAP to bind and stimulate GTPase activity.

RhoA Phosphorylation Does Not Affect Geranylgeranyl Transferase Activity—Incubation of purified cellular membranes with cPKA promotes RhoA extraction from membranes by RhoGDI (13, 20). As non-prenylated RhoA is a cellular PKA target, we analyzed whether cPKA phosphorylation of RhoA impairs addition of a geranylgeranyl moiety as an additional level of regulation. Geranylgeranyl transferase possessed equivalent activity against phosphorylated and control protein GST-RhoA proteins (Fig. 6, A and B). Further, Ser¹⁸⁸ mutants were also comparable substrates (Fig. 6C). Together, these data indicate that phosphorylation of the RhoA tail does not directly alter geranylgeranyl transferase modification of RhoA.

Transient Expression of Ser¹⁸⁸ RhoA Mutants—NIH 3T3 cells transiently transfected with Myc epitope-tagged RhoA, RhoA(S188A), RhoA(S188D), or RhoA(S188E) displayed enhanced stress fibers compared with mock-transfected cells (data not shown), indicating that all transient proteins were functional. The extent of Myc-RhoA GTP loading was evaluated using GST-RBD pulldowns (32). Both phosphoserine-mimetic Myc-RhoA proteins, with Myc-RhoA(S188E) being the more significant, displayed reduced GTP loading in comparison with Myc-RhoA and Myc-RhoA(S188A) proteins (Fig. 7). Myc-RhoA(C190A) proteins were not appreciably GTP-loaded under these conditions and are included as a negative control for GTP loading. These data provide evidence that addition of a negative charge by phosphorylation of Ser¹⁸⁸ is sufficient to negatively regulate RhoA activation.

Stable Expression of Ser¹⁸⁸ RhoA Mutants—To examine whether a functional difference exists between Ser¹⁸⁸ mutant RhoA proteins, stable clones of NIH 3T3 cells expressing Myc-RhoA, Myc-RhoA(S188A), or Myc-RhoA(S188E) were isolated. Two independent clones were chosen for each based solely on expression level and characterized further. Western blots revealed that Myc-RhoA migrates at higher apparent molecular weight than the endogenous RhoA proteins; therefore it was evident that all clones express Myc-RhoA protein at a significantly lower level than endogenous RhoA (Fig. 8A). GST-RBD pulldowns established that, contrary to transiently expressed proteins; there is little or no difference in the GTP-loading profile of stably expressed mutant Myc-RhoA proteins, with the exception of the non-prenylated mutant, Myc-RhoA(C190A) (Fig. 8B).

Activity of Stably Expressed RhoA Protein—As RhoA is hypothesized to antagonize cell spreading (34), NIH 3T3 clones were allowed to spread on fibronectin and collected at the indicated time, and rates of cell spreading were quantified (Fig. 9A). Both Myc-RhoA(S188E) clones spread at a similar rate as a pool of mock-transfected clones, whereas all the Myc-RhoA and Myc-RhoA(S188A) clones spread significantly slower. Additionally, a pool of Myc-RhoA(S188E)-expressing cells (five clones) that express a higher amount of Myc-RhoA (Fig. 9B, inset) still spread significantly faster than a corresponding pool of Myc-RhoA(S188A)-expressing cells (Fig. 9B).

RhoA signaling has been found to antagonize the morpholog-

TABLE II
RhoGDI inhibition of GEF-exchange activity (units $s^{-1} \pm S.D.$)

2 μM GST-RhoA or GST-RhoA serine mutant proteins were incubated with the indicated amount of RhoGDI (GDI) prior to the addition of Vav2. Data are presented as described for Table I. RhoGDI inhibited Vav2-induced nucleotide exchange of phosphomimetic proteins to a greater extent than control proteins. RhoGDI inhibition was more pronounced for GST-RhoA(S188E) than GST-RhoA(S188D).

Condition	wtRhoA	RhoA-S188A	RhoA-S188D	RhoA-S188E
Basal	1.09 \pm 0.11	0.98 \pm 0.12	0.89 \pm .06	0.93 \pm 0.08
150 nM Vav2	6.84 \pm 0.33 (6.3-fold)	6.75 \pm 0.31 (6.9-fold)	6.67 \pm 0.40 (7.4-fold)	6.47 \pm 0.17 (6.9-fold)
+ 0.5 μM GDI	5.74 \pm 0.30 (81%)	5.55 \pm 0.36 (79%)	5.89 \pm 0.22 (86%)	4.50 \pm 0.13 (64%) ^a
+ 1.0 μM GDI	4.27 \pm 0.18 (55%)	4.16 \pm 0.13 (55%)	3.28 \pm 0.19 (41%) ^a	2.89 \pm 0.23 (35%) ^a
+ 2.0 μM GDI	2.74 \pm 0.19 (29%)	2.53 \pm 0.14 (27%)	1.72 \pm 0.12 (14%) ^a	1.53 \pm 0.10 (11%) ^a

^a $p < 0.01$.

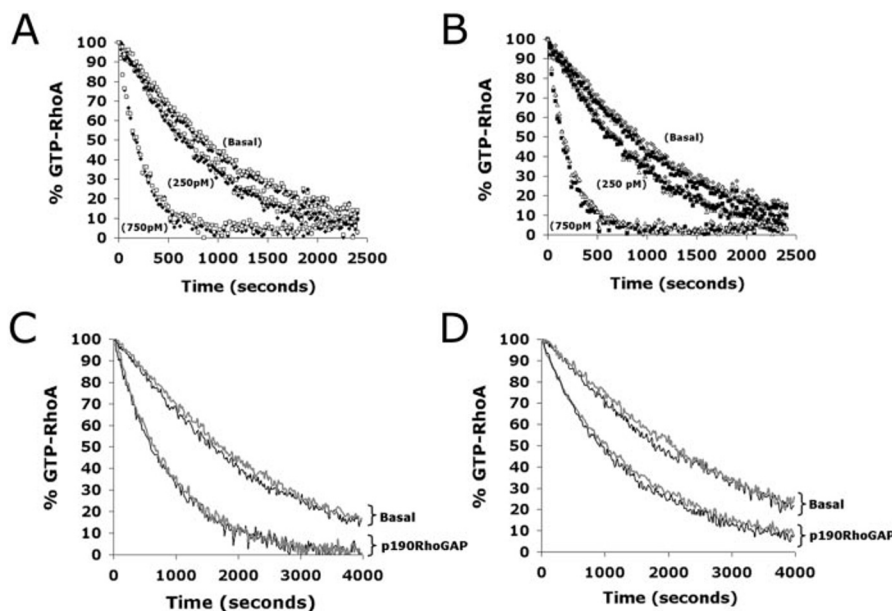


FIG. 5. RhoA phosphorylation does not affect p190RhoGAP activity. *A*, Rho GTPase activity was indirectly examined by incubating cPKA phosphorylated (white symbol) or control GST-RhoA (black symbol) preloaded with GTP in the presence of a coumarin-tagged phosphate-binding protein whose fluorescence increases (465 nm) following binding of phosphate released from GTP. Addition of 250 or 750 μM p190RhoGAP-stimulated GAP activity was not affected by RhoA serine phosphorylation. *B*, GST-RhoA (black symbol), GST-RhoA(S188A) (gray symbol), and GST-RhoA(S188E) (white symbol) were treated as in *A*. The presence of a phosphomimetic residue does not directly influence p190RhoGAP activity. GTP-loaded RhoA (*C*) or GTP-loaded ggRhoA (prenylated) (*D*) were stimulated with p190RhoGAP (500 μM) as indicated. Basal and GAP-induced activity of phosphorylated ggRhoA (gray curves) was consistent with control ggRhoA (black curves). Both basal and stimulated GTPase activities of unmodified RhoA proteins were slightly higher than their prenylated counterparts (basal initial linear velocity (% hydrolysis $min^{-1} \pm S.D.$) of RhoA, phosphorylated RhoA, ggRhoA, and phosphorylated ggRhoA was 1.95 \pm 0.15, 1.66 \pm 0.18, 1.66 \pm 0.17, and 1.50 \pm 0.26, and stimulated was 5.50 \pm 0.40, 5.13 \pm 0.32, 3.96 \pm 0.32, and 3.96 \pm 0.20).

ical affects of cAMP (23); therefore the effects of forskolin on stress fiber organization were examined for the stable clones. Mock-expressing cells revealed dissolution of stress fibers following forskolin activation of adenylate cyclase (Fig. 10, panel above line). A minority of cells expressing wild-type Myc-RhoA were protected from filamentous actin disassembly, whereas cells expressing Myc-RhoA(S188A) were completely protected against the morphological affects of cAMP (Fig. 10, panels below line). On the other hand, both Myc-RhoA(S188E)-expressing clones uniformly displayed stress fiber dissolution (Fig. 10, panels below line). Together, these data provide evidence that addition of a negative charge to Ser¹⁸⁸ by phosphorylation is sufficient to attenuate RhoA activity.

DISCUSSION

In agreement with previous work (13, 19, 23), we found that RhoA is an excellent substrate for PKA. Additionally, we discovered that RhoG, but not Cdc42 or Rac1, was also phosphorylated by PKA. Although RhoA, RhoG, and Cdc42 possess carboxyl serine residues, the preceding three amino acids that target PKA diverge. Although RhoA, Rap1a, and Rap1b, all contain three lysines (KKKS), Cdc42 (PKKS) contains a proline turn in place of the initial basic residue, a divergence that may

explain why Cdc42 is a poorer substrate than RhoA *in vitro* (33). On the other hand, RhoG (KRGRS) contains a glycine flanked by three basic residues, a motif more consistent with KKKS. The significance of RhoG phosphorylation is unknown and currently under investigation.

Unlike Rap1a and Rap1b, which are easily isolated as phosphoproteins from cells (15, 16), a clear demonstration of intracellular RhoA phosphorylation is lacking. Lang *et al.* (13) were able to immunoprecipitate only small amounts of ³²P-labeled RhoA from intact cells, whereas Essler *et al.* (38) reported recently that a significant charge shift of RhoA was not observed following cAMP stimulation of HUVEC cells. To address this problem, we created antibodies that specifically recognize the phosphorylated form of RhoA. When expressed in cells, the non-prenylated RhoA (C190A) was a cellular target of PKA following forskolin stimulation and during cell spreading, an event associated with low RhoA (32, 34) and high PKA activity (35, 36). Although limited by antibody constraints, these results provide the first conclusive evidence, at least in the case of non-prenylated RhoA, that Ser¹⁸⁸ is phosphorylated in response to cellular PKA activation *in vivo*.

Treatment of cells with cAMP or cGMP agonists is associated

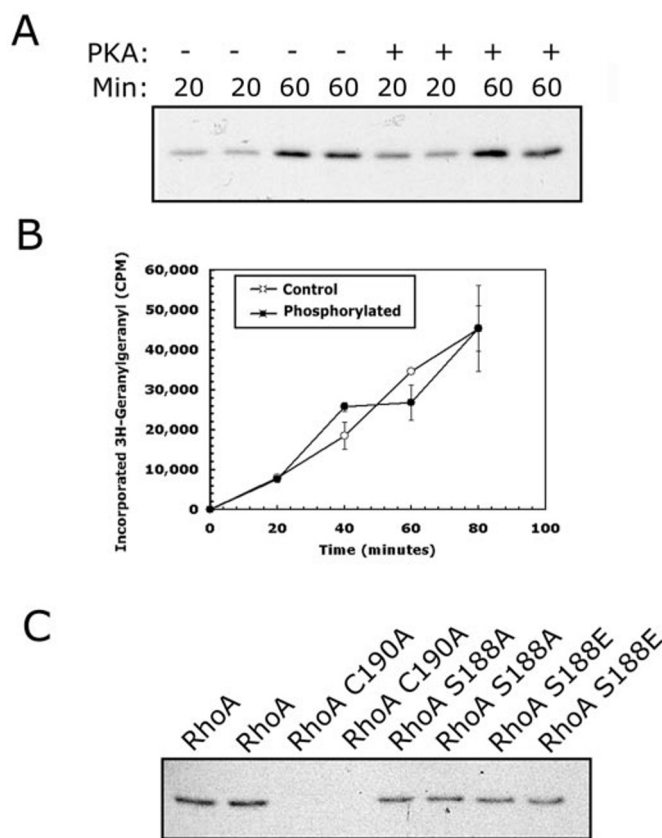


FIG. 6. RhoA phosphorylation does not affect geranylgeranyl transferase activity. *A*, duplicate phosphorylated or control GST-RhoA were incubated with ³H-geranylgeranyl pyrophosphate and geranylgeranyl transferase for 20 or 60 min, and the extent of prenylation was visualized by SDS-PAGE followed by autoradiography. *B*, GST-RhoA-Sepharose was phosphorylated as described under "Experimental Procedures" and then incubated with ³H-geranylgeranyl pyrophosphate and geranylgeranyl transferase for the indicated times and then repeatedly washed, and the extent of prenylation was calculated by measuring radiation counts released per min. Values represent two independent reactions \pm S.D. *C*, duplicate samples of GST-RhoA, GST-RhoA(C190A) (cannot be prenylated), and GST-RhoA Ser¹⁸⁸ mutants were incubated with ³H-geranylgeranyl pyrophosphate and geranylgeranyl transferase for 20 min, and the extent of prenylation was visualized by SDS-PAGE followed by autoradiography.

with translocation of RhoA from membranes (13, 14). Non-prenylated RhoA is efficiently phosphorylated within the cell (Fig. 2), suggesting that it may be a target of PKA regulation. We therefore analyzed whether Ser¹⁸⁸ phosphorylation controls RhoA cycling by impeding prenylation. *In vitro* assays demonstrated that geranylgeranyl transferase activity was not sensitive to the presence of a phosphate on Ser¹⁸⁸. As events of Rho protein prenylation are poorly understood, it remains possible that phosphorylation of this residue affects post-translational modification of RhoA through mechanisms not reflected by *in vitro* assays. However, regulating RhoA cycling at the step of prenylation appears to be an inefficient and long term approach for a kinase that depends on localized and transient activity (reviewed in Ref. 39).

We found that transiently expressed phosphomimetic Myc-RhoA proteins were poorly loaded with GTP nucleotides compared with control proteins. We also demonstrated that Myc-RhoA(S188E) protein signaling is significantly attenuated compared with control proteins and that this difference was not reflected in the GTP-loading profiles of stably transfected cells. Both of these results are consistent with enhanced sequestration of Myc-RhoA(S188E) by RhoGDI. In the case of transiently expressed protein, sequestration by RhoGDI would reduce the

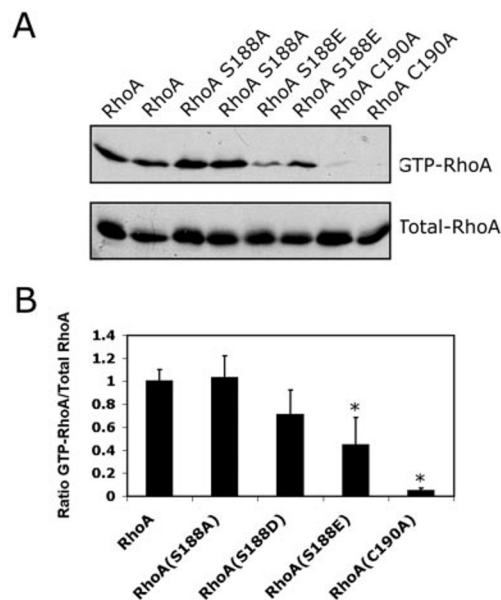


FIG. 7. GTP loading of transiently expressed Myc-RhoA proteins. *A*, the indicated Myc-RhoA proteins were transiently transfected in duplicate for each protein and then collected and processed for GTP loading as described under "Experimental Procedures." *B*, three individual experiments done in duplicate were scanned and quantified by densitometry as described under "Experimental Procedures." The ratios of GTP-loaded Myc-RhoA to total Myc-RhoA were normalized to wild-type Myc-RhoA values. Error bars denote standard deviation of GTP loading (*, $p < 0.01$ compared with wild-type and Myc-RhoA(S188A) proteins).

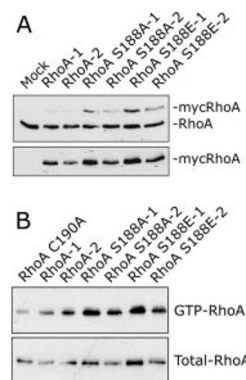


FIG. 8. Evaluation of NIH 3T3 cells stably expressing Myc-RhoA protein. Two isolated clones were chosen for each Myc-RhoA protein based on expression level. *A*, upper panel, lysates were collected from the indicated clone and Western blotted with an anti-RhoA monoclonal antibody. Myc-RhoA migrated at a higher molecular weight in 20% SDS-PAGE gels and was expressed at considerably lower amounts than endogenous RhoA. Lower panel, the above blot was stripped and re-probed with an anti-Myc antibody. *B*, stable Myc-RhoA clones were collected and processed for GTP-loading profiles. GST-RBD pulldowns were blotted with the anti-Myc antibody to specifically show loading of exogenous Myc-RhoA protein. Unlike during transient expression conditions, GTP loading of Myc-RhoA(S188E) proteins were comparable with Myc-RhoA(S188A) proteins. Myc-RhoA(C190A) had a depressed level of GTP loading compared with other RhoA proteins.

accessibility of GEFs, as is observed *in vitro* (Tables I and II). In the case of stably expressed proteins, Myc-RhoA(S188E) that has become GTP-loaded over time could still be aberrantly sequestered by RhoGDI. This would be reflected by low RhoA activity in the cell (see Figs. 9 and 10) but not by RBD pulldowns because of a limitation of the assay. The lysis conditions of RBD pulldown assays requires disruption of both RhoA(GTP)-membrane and RhoA(GTP)-effector complexes to form RhoA(GTP)-GST-RBD complexes that are driven by the vast molar excess of GST fusion

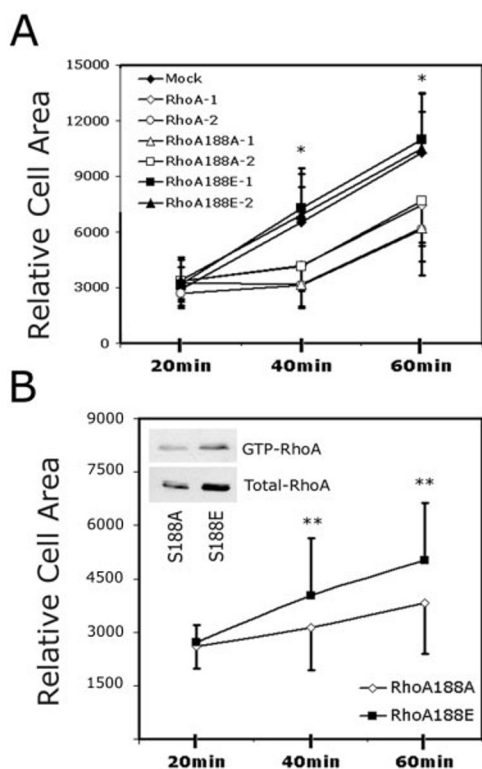


FIG. 9. Spreading profiles of Myc-RhoA-expressing clones. *A*, the indicated Myc-RhoA clones were allowed to spread on fibronectin, and the extent of cell spreading was quantified. Myc-RhoA and Myc-RhoA(S188A) clones spread slower than mock-transfected clones or the two Myc-RhoA(S188E) clones (*, $p < 0.01$). *B*, five Myc-RhoA(S188A) clones or five Myc-RhoA(S188E) clones were pooled, and the rate of cell spreading on fibronectin was calculated. The pool of Myc-RhoA(S188E) clones spread more rapidly than Myc-RhoA(S188A) cells (**, $p < 0.02$), although GTP-loaded Myc-RhoA levels were higher in the Myc-RhoA(S188E)-expressing cells (panel inset as indicated).

protein. Not unexpectedly, we found that the lysis conditions completely disrupt RhoA-RhoGDI complexes,² and have been unable to find lysis conditions that liberate RhoA(GTP) for RBD pulldown assays and preserve RhoA-RhoGDI binding. It is probable, therefore, that a portion of the stably expressed and GTP-loaded Myc-RhoA(S188E) protein is released from inactive RhoA(GTP)-RhoGDI pools, in addition to active RhoA(GTP)-effector complexes. Thus, GST-RBD pulldowns, while an effective tool for measuring RhoGAP-mediated inhibition (34) or GEF activation of RhoA (31), will not reflect RhoGDI inhibition by sequestration.

In addition to enhanced binding to RhoGDI, Myc-RhoA(S188E) proteins may have lower binding affinity to an effector, such as Rho kinase (23). However, we found that constitutively active GST-RhoA(63L, S188E) was as efficient as GST-RhoA(63L, S188A) proteins in pulling down Rho kinase from NIH cell lysates.³ Further, stably expressed phosphomimetic RhoA proteins bound the RBD domain of the Rho effector Rhotekin (Fig. 8B). Therefore, we propose that attenuation of phosphomimetic RhoA activation and activity is because of cytosolic sequestration of RhoA driven by enhanced RhoGDI interactions that are observed *in vitro*.

The data presented here provide information regarding RhoA phosphorylation in context of regulatory protein interactions and demonstrate that the addition of a negative charge to Ser¹⁸⁸ is sufficient to diminish both RhoA activation and activ-

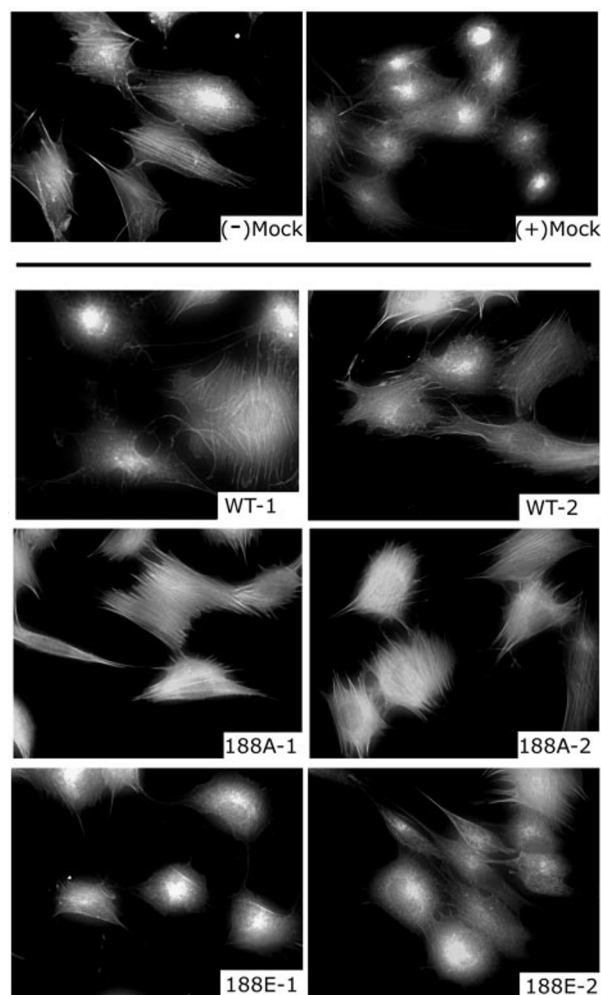


FIG. 10. Myc-RhoA(S188E) clones are sensitive to forskolin. *Panel above line*, mock-transfected NIH 3T3 cells attached to fibronectin-coated coverslips were incubated for 20 min in serum-free medium containing Me₂SO vehicle ((-) *Mock*) or 25 μ M forskolin ((+) *Mock*). *Panels below line*, the indicated NIH 3T3 clones were treated with 25 μ M forskolin and then fixed and stained with phalloidin to identify filamentous actin.

ity within the context of a cell. As PKA also uncouples GEF activation from receptor stimulation (26, 37) and antagonizes microfilament integrity by directly phosphorylating and inhibiting myosin light chain kinase (40), it is becoming clear that PKA inhibits RhoA signaling pathways at multiple levels. It will be important in future work to establish where and when RhoA phosphorylation occurs within the cell and to address whether PKA phosphorylation works in parallel with RhoGAP-mediated inhibition of RhoA during events of cell protrusion and migration.

Acknowledgments—We thank Drs. David Siderovski and Adam Shutes for technical assistance in the preparation of phosphate-binding protein, Christy Barlow for technical assistance in preparation of GST-RBD, and the collaborators mentioned under “Experimental Procedures” for providing reagents.

REFERENCES

- Bishop, A. L., and Hall, A. (2000) *Biochem. J.* **348**, 241–255
- Schmidt, A., and Hall, A. (2002) *Genes Dev.* **16**, 1587–1609
- Gamblin, S. J., and Smerdon, S. J. (1998) *Curr. Opin. Struct. Biol.* **8**, 195–201
- Kimura, K., Ito, M., Amano, M., Chihara, K., Fukata, Y., Nakafuku, M., Yamamori, B., Feng, J., Nakano, T., Okawa, K., Iwamatsu, A., and Kaibuchi, K. (1996) *Science* **273**, 245–248
- Amano, M., Ito, M., Kimura, K., Fukata, Y., Chihara, K., Nakano, T., Matsura, Y., and Kaibuchi, K. (1996) *J. Biol. Chem.* **271**, 20246–20249
- Watanabe, N., Kato, T., Fujita, A., Ishizaki, T., and Narumiya, S. (1999) *Nat. Cell Biol.* **1**, 136–143

² S. M. Ellerbroek and K. Burridge, unpublished results.

³ S. M. Ellerbroek and K. Burridge, unpublished results.

7. Lang, P., Gesbert, F., Thiberge, J., Troalen, F., Dorseuil, O., Gacon, G., and Bertoglio, J. (1993) *Biochem. Biophys. Res. Commun.* **196**, 1522–1528
8. Michaelson, D., Silletti, J., Murphy, G., D'Eustachio, P., Rush, M., and Phillips, M. R. (2001) *J. Cell Biol.* **152**, 111–126
9. Hori, Y., Kikuchi, A., Isomura, M., Katayama, M., Miura, Y., Fujioka, H., Kaibuchi, K., and Takai, Y. (1991) *Oncogene* **6**, 515–522
10. Allal, C., Favre, G., Couderc, B., Salicio, S., Sixou, S., Hamilton, A. D., Sebti, S. M., Lajoie-Mazenc, I., and Pradines, A. (2000) *J. Biol. Chem.* **275**, 31001–31008
11. Olofsson, B. (1999) *Cell. Signal.* **11**, 545–554
12. Gosser, Y. Q., Nomanbhoy, T. K., Aghazadeh, B., Manor, D., Combs, C., Cerione, R. A., and Rosen, M. K. (1997) *Nature* **387**, 814–819
13. Lang, P., Gesbert, F., Delespine-Carmagnat, M., Stancou, R., Pouchelet, M., and Bertoglio, J. (1996) *EMBO J.* **15**, 510–519
14. Sawada, N., Itoh, H., Yamashita, J., Doi, K., Inoue, M., Masatsugugu, K., Fukunaga, Y., Sakaguchi, S., Sone, M., Yamahara, K., Yurugi, T., and Nakao, K. (2001) *Biochem. Biophys. Res. Commun.* **280**, 798–805
15. Quilliam, L. A., Mueller, H., Bohl, B. P., Prossnitz, V., Sklar, L. A., Der, C. J., and Bokoch, G. M. (1991) *J. Immunol.* **147**, 1628–1635
16. Lerosey, I., Pizon, V., Tavitian, A., and de Gunzburg, J. (1991) *Biochem. Biophys. Res. Commun.* **175**, 430–436
17. Hu, C. D., Kariya, K., Okada, T., Qi, X., Song, C., and Kataoka, T. (1999) *J. Biol. Chem.* **274**, 48–51
18. Ribeiro-Neto, F., Urbani, J., Lemee, N., Lou, L., and Altschuler, D. L. (2002) *Proc. Natl. Acad. Sci. U. S. A.* **99**, 5418–5423
19. Forget, M. A., Desrosiers, R. R., Gingras, D., and Beliveau, R. (2001) *Biochem. J.* **361**, 243–254
20. Kwak, J. Y., and Uhlinger, D. J. (2000) *Biochem. Biophys. Res. Commun.* **267**, 305–310
21. O'Connor, K. L., Nguyen, B. K., and Mercurio, A. M. (2000) *J. Cell Biol.* **148**, 253–258
22. Faucheux, N., and Nagel, M. D. (2002) *Biomaterials* **23**, 2295–2301
23. Dong, J. M., Leung, T., Manser, E., and Lim, L. (1998) *J. Biol. Chem.* **273**, 22554–22562
24. Sauzeau, V., Le Jeunne, H., Cario-Toumaniantz, C., Smolenski, A., Lohmann, S. M., Bertoglio, J., Chardin, P., Pacaud, P., and Loirand, G. (2000) *J. Biol. Chem.* **275**, 21722–21729
25. Gratacap, M. P., Payrastre, B., Nieswandt, B., and Offermanns, S. (2001) *J. Biol. Chem.* **276**, 47906–47913
26. Manganello, J. M., Huang, J. S., Kozasa, T., Voyno-Yasenetskaya, T. A., and Le Breton, G. C. (2003) *J. Biol. Chem.* **278**, 124–130
27. Gudi, T., Chen, J. C., Casteel, D. E., Seasholtz, T. M., Boss, G. R., and Pilz, R. B. (2002) *J. Biol. Chem.* **277**, 37382–37393
28. Brune, M., Hunter, J. L., Howell, S. A., Martin, S. R., Hazlett, T. L., Corrie, J. E., and Webb, M. R. (1998) *Biochemistry* **37**, 10370–10380
29. Khosravi-Far, R., and Der, C. J. (1995) *Methods Enzymol.* **255**, 46–60
30. Leonard, D. A., Evans, T., Hart, M., Cerione, R. A., and Manor, D. (1994) *Biochemistry* **33**, 12323–12328
31. Arthur, W. T., Ellerbroek, S. M., Der, C. J., Burrige, K., and Wennerberg, K. (2002) *J. Biol. Chem.* **277**, 42964–42972
32. Ren, X. D., Kiosses, W. B., and Schwartz, M. A. (1999) *EMBO J.* **18**, 578–585
33. Feoktistov, I., Goldstein, A. E., and Biaggioni, I. (2000) *Mol. Pharmacol.* **58**, 903–910
34. Arthur, W. T., Petch, L. A., and Burrige, K., (2000) *Curr. Biol.* **10**, 719–722
35. Dormond, O., Bezzi, M., Mariotti, A., and Ruegg, C. (2002) *J. Biol. Chem.* **277**, 45838–45846
36. O'Connor, K. L., and Mercurio, A. M. (2001) *J. Biol. Chem.* **276**, 47895–47900
37. Laudanna, C., Campbell, J. J., and Butcher, E. C. (1997) *J. Biol. Chem.* **272**, 24141–24144
38. Essler, M., Staddon, J. M., Weber, P. C., and Aepflebacher, M. (2000) *J. Immunol.* **164**, 6453–6549
39. Feliciello, A., Gottesman, M. E., and Avvedimento, E. V. (2001) *J. Mol. Biol.* **308**, 99–114
40. Lamb, N. J., Fernandez, A., Conti, M. A., Adelstein, R., Glass, D. B., Welch, W. J., and Feramisco, J. R. (1988) *J. Cell Biol.* **10**, 1955–1971